ACTA PHYSICA POLONICA A No. 4 Vol. **148** (2025)

Dual Phosphorescence of Rhodamine B Lactone

J. Karpiuk* and E. Karpiuk

Institute of Physics, Polish Academy of Sciences, al. Lotników, 32/46, PL-02-668 Warsaw, Poland

Received: 10.11.2025 & Accepted: 11.12.2025

Doi: 10.12693/APhysPolA.148.284

*e-mail: jkarpiuk@ifpan.edu.pl

Rhodamines are well-known as highly coloured dyes and potent, bright fluorophores with negligible phosphorescence, and thus often neglected triplet states. Rhodamines with a carboxyphenyl group exist in spirocyclic lactone and as open-ring colour zwitterion or cation forms. The colourless lactone is virtually the only form of rhodamines in aprotic environment and, upon ultraviolet photoexcitation at room temperature, it undergoes ultrafast intramolecular electron transfer and emits — depending on solvent polarity — single or dual fluorescence from a charge-transfer state and zwitterion populated upon adiabatic photodissociation of the C–O bond. The photophysics and mechanisms of complex excited state processes in rhodamine lactones are still poorly understood, and especially the nature of nonradiative deactivation and the role of triplet states remain unknown. Here, we present a photophysical study of rhodamine B lactone in rigid organic solvent glasses at 77 K and report highly efficient phosphorescence generated by intramolecular charge transfer, demonstrating the potential of rhodamine lactones for triplet generation by charge recombination. A mechanism behind the formation of triplet states in rhodamine lactones is proposed.

topics: dual phosphorescence, rhodamine B lactone (LRB), triplet generation by charge recombination, photoinduced electron transfer in spirocyclic molecule

1. Introduction

Early research on the photophysics and luminescence of organic molecules often considered electronic excited triplet states as undesired dark products of singlet state deactivation. Recent studies increasingly indicate that, due to the spin-forbidden nature of their decay to the ground state, triplets can act as a long-lived energy storage and play fundamental role in physical, chemical or biological processes, including photon upconversion [1], charge separation [2], room temperature phosphorescence [3], or organic photovoltaics [4]. Controlled generation of triplet states in heavy-atom free organic molecules is gaining in importance and stimulates demand for suitable molecular structures and efficient mechanisms of triplet state population. One of such mechanism is the formation of triplet by intramolecular charge recombination in molecular donor–acceptor (D–A) systems [5].

An interesting class of molecules in this context are D–A dyads with D and A moieties linked by an sp^3 carbon atom [6, 7]. Due to the rigid locking of the D and A moieties and the orthogonal D–A geometry, they enable intramolecular non-covalent interactions (e.g. homo- or spiroconjugation) and efficient coupling of electron orbital angular momentum with spin. An attractive exemplification of such systems are spirocyclic rhodamine lactones (LR); these are neutral molecular forms of rhodamines [8] with a carboxyphenyl group, which can be easily obtained in a crystalline solid form and, as such, exist virtually for unlimited time. When dissolved in aprotic solvents, both nonpolar and polar, the lactone (L) form produces colourless solutions. Protic solvents induce the opening of the lactone ring and stabilize the intensely coloured zwitterion (Z) form. The position of the L ↔ Z equilibrium depends upon the rhodamine–solvent hydrogen bonding and the dielectric properties of the solvent [9]. Protonation of the carboxyphenyl group converts the zwitterion into the cation (C) form of rhodamine with the principal chromophore identical as in the Z form (see Fig. 1).

Colour forms of rhodamines are among the most frequently studied and used organic fluorophores [10]. Historically, the interest in these dyes had been driven by their applications as laser dyes [11], fluorescence and chemosensors [12], bioimaging probes [13], or photoactivatable fluorophores for high-resolution optical nanoscopy [14]. The photophysics of rhodamines have been extensively studied [15, 16], and the effects of structure, environment and temperature on the excited-state

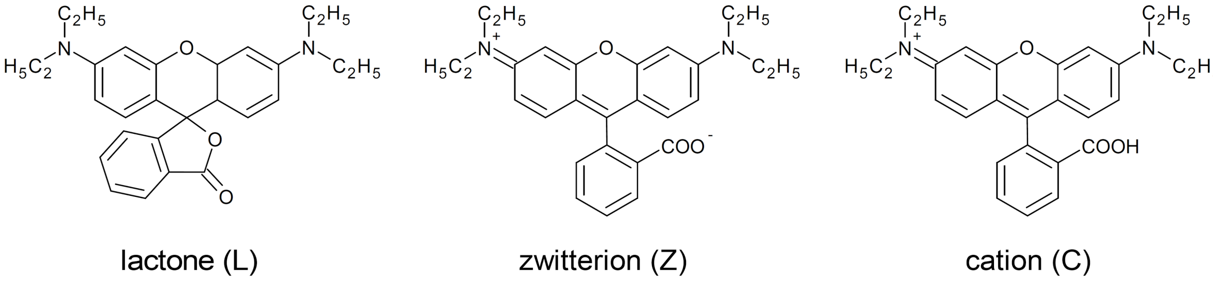

Fig. 1. Molecular forms of rhodamine B: lactone (L), zwitterion (Z), and cation (C).

properties of the Z and C forms are relatively well understood. The general perception is that these open-ring forms of rhodamines are characterized by high fluorescence quantum yields, photostability and low yields of triplet formation [17–19].

In contrast to the Z and C forms of rhodamines, the photophysics and excited state properties of rhodamine lactones are largely unknown, which often leads to incorrect description of spirocyclic rhodamine lactones or lactams as nonfluorescent forms of rhodamines [12]. As a matter of fact, however, rhodamine B lactone (LRB) or rhodamine 101 lactone (LR101) in medium polar aprotic solvents emit fluorescence with quantum yields of a few percent [20, 21] and represent an unique example of adiabatic photochemistry involving two emitting excited states, one of which is populated through excited-state dissociation. Accordingly, in sufficiently polar environment, LR display dual fluorescence from

- a highly polar charge transfer (CT) state of the L form ($^1\mathrm{L}_{\mathrm{CT}}$), populated upon electron transfer (ET) from the xanthene (X) to the phthalide (PD) moiety (see Fig. 1; this polar CT state has the dipole moment of $\mu_e = 25$ D in LRB [20] and $\mu_e = 26$ D in LR101 [21]),
- an excited state of the open-ring Z form (^{1}Z) produced in the course of the photoexcited Franck–Condon state relaxation by C–O bond cleavage in the lactone ring [20–22].

The branching into deactivation pathways ultimately leading to the emitting states occurs in non-relaxed vibronic levels, and the lack of the kinetic correlation between the fluorescence decays of the $^1\mathrm{L}_{\mathrm{CT}}$ and ^{1}Z states proves that the fluorescent states do not communicate with each other, are not in equilibrium, and deactivate without any effect on each other [21]. The $^1\mathrm{L}_{\mathrm{CT}}$ state relaxes to the ground state mainly by radiative and nonradiative back ET, while the decays of the ^{1}Z state have been found to strongly depend on the solvent and temperature [23]. At 77 K, a beautiful, deeply red, long-lived phosphorescence was observed for LR101 [24]. The high quantum yield of LR101 phosphorescence (0.72) indicated the major role of intersystem crossing (ISC) in lactone photophysics, which clearly suggests a highly efficient ISC mechanism and its close relationship to intramolecular charge separation and recombination in the specific spirocyclic structure.

The early research on the photophysics of LR has thus raised a number of important questions that still remain unanswered. These include, inter alia, (i) the nature of the photoexcited Franck–Condon state and the mechanism of ultrafast primary ET in liquid and solid environment, (ii) the anomalously large Stokes shift of L fluorescence and the related pathways of energy dissipation, (iii) the mechanism of branching into the $^1\mathrm{L}_{\mathrm{CT}}$ and ^{1}Z relaxation pathways in the non-relaxed excited state, (iv) the mechanisms of nonradiative deactivation of the $^1\mathrm{L}_{\mathrm{CT}}$ and ^{1}Z states and, last but not least, (v) the nature and source of the highly efficient phosphorescence of LR and the mechanism of intersystem crossing processes.

Here, we address some of these questions and report the photophysics of LRB in organic solvent glasses at 77 K. Our study shows that under these conditions LRB continues to display dual fluorescence from the $^1\mathrm{L}_{\mathrm{CT}}$ and ^{1}Z states and, similarly to LR101, it emits high intensity red phosphorescence. Using time-resolved emission spectroscopy in the time range from μs to s, we are able to show that LRB emits also another short-wave phosphorescence. As a result, the total LRB luminescence in glasses at 77 K comprises dual fluorescence and dual phosphorescence from two structurally different singlet and two structurally different triplet states, associated with different chromophores within the LRB molecule. The emitting singlets are populated in a branching occurring in vibrationally non-relaxed states. The branching is faster than the internal conversion, and in this sense the observed emissions result from the violation of the Kasha rule [25]. The emitting triplet states are populated in different kinetically non-correlated ISC processes based on two different ISC mechanisms. Comparison with triarylmethane lactones [26] and their diaryl analogues [27] allows us to shed light on the structure–property relationship underlying the complex photophysics and to explain the role of charge separation and recombination in population of triplet states in rhodamine lactones.

2. Materials and methods

The lactone form of rhodamine B has been prepared by two methods, i.e., (i) the one described by Klein and Hafner using the rhodamine B chloride salt [20] and (ii) by crystallisation of rhodamine B base (Aldrich) from cyclohexane. Both materials showed identical absorption and fluorescence spectra at room temperature (RT), and finally, the material obtained by method (ii) was used in this study.

The experimental results were obtained in solvents: methylcyclohexane (MCH, Aldrich, spectrophotometric grade) was passed through a column filled with freshly activated SiO_2; 2-methyltetrahydrofurane (MTHF, Aldrich, anhydrous) and acetonitrile (ACN, Merck, for spectroscopy) were used as received; butyronitrile (BTN, Merck, for synthesis) was twice distilled over $KMnO_4 + K_2CO_3$ and P_2O_5.

Absorption spectra were recorded with a Shimadzu UV-2700 spectrophotometer. Steady-state luminescence spectra were recorded with a Fluorolog-3 (Horiba Jobin Yvon) spectrofluorimeter and subsequently corrected for the spectral response of the detection systems and, additionally, for the solvent effects (e.g. Raman lines, second order effects of the excitation line). Luminescence spectra were recorded as a function of wavelength and subsequently multiplied by the factor λ^2 to convert counts per wavelength into counts per wavenumber. This representation of the luminescence spectra is preferred as it allows direct visualization of energy relationships/differences in broad spectral regions. All luminescence measurements were carried out using solutions deoxygenated by purging with high-purity nitrogen (typically for 30 min).

Fluorescence decays were recorded with a Delta Hub time-correlated single-photon counting (TC SPC) timing module and a DeltaDiode excitation source (303 nm) coupled to Fluorolog-3 and analyzed using the DAS6 decay analysis software (practical time resolution 0.2 ns). Time-resolved phosphorescence measurements were carried out with a FL-1040 phosphorimeter accessory, using a xenon flash lamp as the excitation source. Though the full-width half-maximum of the flash lamp's pulse is 3 μs, a minimum initial delay time of 50 μs was used to separate fluorescence from phosphorescence and avoid any interference from prompt fluorescence. Signal gating procedures were performed using the spectrofluorimeter control electronics and the FluoroEssence software.

The concentrations of LRB were between 2.5×10^{-6} M and 3.0×10^{-6} M, which excluded aggregation [15]. Luminescence spectra were recorded for optically transparent rigid solutions (glasses) of excellent quality (MCH and MTHF) or with only small amount of cracks (BTN) in the area illuminated by the excitation beam. The luminescence quantum yields at 77 K were determined as described earlier in [28], using the same molar absorptivity at 77 K as at 298 K and making appropriate corrections for changes in concentrations and refractive indices.

3. Results

3.1. Absorption and fluorescence at 298 K

Unlike the Z and C forms, the rhodamine B lactone molecule does not comprise any chromophore with absorption transitions in the visible range, and therefore any absorption of the L form solution in an aprotic solvent in the range 17000–20000 cm^{-1} (500–588 nm) would indicate the presence of the Z or C forms in the ground state. The Z form would emerge from a possible ground state L ↔Z equilibrium, while the C form could be only the product of lactone ring opening and protonation by traces of protic substances, possibly present in small amounts in more polar (formally) aprotic solvents. In our measurements, LRB solutions in MTHF and BTN at 298 K showed no visible absorption within the sensitivity of the absorption spectrophotometer (0.001 absorbance unit) at the lactone concentration $c_{\rm L} = 2.5 \times 10^{-6}$ M, which — assuming molar absorptivities for the L form of 15800 M^{-1} cm^{-1} in acetonitrile [20] and for the C form of 130000 M^{-1} cm^{-1} [9], — translates into $c_{\rm C} \leq 0.8 \times 10^{-8}$ M, indicating that at RT the Z or C concentrations, if any, were less than 0.3% relative to the concentration of L. Although this conclusion holds also for the C form at 77 K, the appearance of the Z form in the lactone solution at 77 K glass cannot be excluded because of a possible temperature-dependent shift of the ground state L ↔ Z equilibrium towards the Z form or due to other factors (*vide infra*).

The absence of visible absorption in LRB solutions in BTN (dielectric constant $\varepsilon = 20.7$) at RT does not agree with the results of El-Rayyes et al. [29], who reported that in polar solvents ($\varepsilon > 15$) the solutions were red, indicating the opening of the lactone ring and the formation of the quinoid (cationic) C form in the ground state, and — in this context — points to the critical importance of checking solvents for the presence of trace protic impurities in studies on rhodamine lactones. In fact, we found that LRB can be successfully used as a sensitive sensor for detecting protic substances in polar aprotic solvents and routinely used it to verify their presence in our research.

Additional complication in assessing the concentrations of colour forms in low polar aprotic solvents could be a residual absorption due to a coloured complex forming in contact with the silica cell windows, while rhodamine B (RB) in the bulk solution remains in the colourless L form [15]. We observed such phenomenon for solution of LRB in

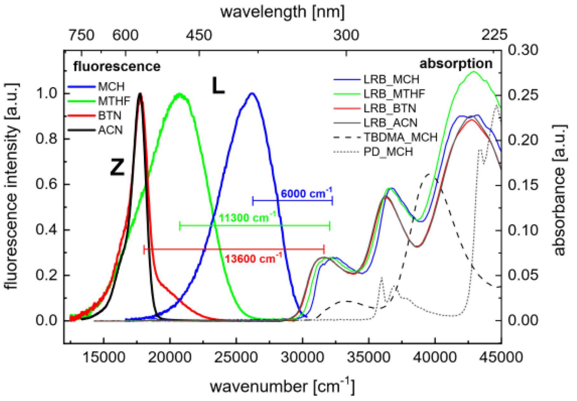

Fig. 2. Absorption (thin lines) and fluorescence (thick lines) spectra of LRB in MCH, MTHF, BTN and ACN at 298 K, $\tilde{\nu}_{exc} = 32470$ cm^{-1} (308 nm), with absorption spectra of 4-t-butyl-N,N-dimethylaniline (TBDMA, dashed line) and phthalide (PD, dotted line) in MCH. Horizontal lines show Stokes shifts of LRB in MCH, MTHF, and BTN.

cyclohexane at room temperature, where transfer of the solution from one silica absorption cell to another resulted in a blue shift of the visible absorption peak at 18380 cm^{-1} (554 nm) to 18210 cm^{-1} (549 nm) and its decrease by more than twice with almost no change in the ultraviolet (UV) absorption of the L form at 32350 cm^{-1} (309 nm).

Figure 2 shows the absorption spectra of LRB, normalized to the maximum of the first absorption band, and the fluorescence spectra in MCH, MTHF, BTN, and ACN at 298 K. The UV absorption spectrum of LRB is composed of three bands with maxima in MCH at 32250, 36760 and 42020 cm^{-1} (310, 272 and 238 nm, respectively). The first two bands show a red shift with increasing solvent polarity, while the third band — a blue one.

Upon photoexcitation at 298 K, in low and medium polar aprotic solvents (MCH and MTHF), LRB displays short-wave single-band (L) fluorescence with quantum yield ranging from 0.0085 (MCH) to 0.07 (MTHF), while in polar solvents a second band (Z) appears; the quantum yield of the L band decreases with simultaneous increase of the Z band [20, 23]. The L and Z bands are assigned to the closed and open ring forms, respectively [20–23]. The most intriguing conclusions from the comparison of absorption and fluorescence spectra of LRB in solvents of different polarities at RT concern the large positive solvatofluorochromism of at least 8200 cm^{-1} between MCH and BTN, and the large Stokes shift of 6000 cm^{-1} in MCH, increasing to 11300 cm^{-1} in MTHF and to at least 13600 cm^{-1} in BTN (the maximum of the L fluorescence band in BTN is difficult to estimate due to the overlap with the Z band). Although somewhat smaller than that originally reported by Klein and Hafner [20] for LRB in cyclohexane (7150 cm^{-1}), the large Stokes shift in the nonpolar solvent clearly indicates that the photoexcited state is not the source of the observed L fluorescence, raising the question about the nature of the Franck–Condon state populated in LRB absorption.

In an attempt to address the question, the electronic absorption transitions in LRB were explored by Sinel'nikov and Artyukhov [30] with a semi-empirical method (INDO — Intermediate Neglect of Differential Overlap) and by Mchedlov-Petrossyan et al. [31] with *ab initio* (b3lyp/cc-PVDZ) chemical quantum calculations. Both mentioned approaches suggested significant contributions from CT transitions ("full charge transfer") in the low-energy absorption band of LRB involving direct electron transfer from the xanthene part to the phthalide moiety. Although the slightly positive solvatochromism of this band (700 cm^{-1} between MCH and ACN), resembling that observed for LR101 [21], indicates a contribution from CT transition(s), the experimentally determined values of the molar absorption coefficients (13700 and 12400 M^{-}1 cm^{-l} for LRB [20] in cyclohexane and LR101 in MTHF [21], respectively) are incompatible with the low computed oscillator strengths (< 0.01) of the $S_0 \rightarrow S_1$ and $S_0 \rightarrow S_2$ transitions, as, in fact, admitted by the authors [31]. Therefore, CT transition(s) can account only for a minor fraction of the LRB absorption and do not contribute significantly to the population of the photoexcited Franck–Condon state.

The LRB molecule geometrically consists of two perpendicular parts [32], comprising three non-conjugated chromophores: two electron-rich N,N-diethylaminophenyls (DEA) linked by an oxygen atom and a spiro carbon atom to form tricyclic diethylaminoxanthene, and a third one represented by an electrophilic phthalide (PD) moiety. The oxygen atom irrelevantly participates in the formation of the low-energy transitions in the electronic spectrum of LRB [31], and the spiro carbon atom effectively decouples the π-electronic systems of DEA and PD moieties [21]. The absorption spectra of LR show distinct dependence on the alkylamino substituents [21, 23], and the positions and shapes of the two low energy absorption bands resemble those observed in the absorption spectra of corresponding aminophenyls [33], as exemplified by 4-t-butyl-N,N-dimethylaniline (TBDMA) (Fig. 2). This indicates weak interactions between DEA and PD chromophores of LRB. The low level of electronic conjugation in the ground state between the three chromophores is also compatible with the additivity of electronic transitions observed in the structurally related triarylphenylmethane lactones [27, 34]. Considering the above, it can be assumed that the photoexcited Franck–Condon state in LRB is to a large extent localized on one of the aminophenyl chromophores.

3.2. Steady-state luminescence at 77 K

LRB was studied at 77 K in three organic solvent glasses: BTN, MTHF, and MCH. The luminescence spectra of LRB in BTN at 77 K consists substantially of three bands: a low intensity broad short-wave (L) band emitted in the 17000–25000 cm^{-1} range, and two narrower, high intensity bands in the 17000–19000 cm^{-1} (I band) and 13000–16000 cm^{-1} (R band) ranges (spectrum A, Fig. 3). The shapes of the L and R bands do not depend on the excitation energy, while the I band changes both its shape and its intensity relative to the R band depending on the excitation energy.

A more detailed examination shows that the I band observed in the BTN glass is composed of two bands, peaking at 17850 and 18400 cm^{-1}. The 17850 cm^{-1} band (spectrum B, Fig. 3) is the only band in the luminescence spectrum obtained with the excitation energy below the red edge of the lowest lactone absorption band (28570 cm^{-1}, 350 nm), and as such it must be emitted upon excitation of a ground state species other than the lactone, i.e., the Z or C form. The luminescence excitation spectrum recorded at $\tilde{\nu}_{obs} = 17850$ cm^{-1} (Fig. 4) differs from the absorption spectrum of the C form obtained by protonation of LRB in acetonitrile [9], and therefore the 17850 cm^{-1} band is interpreted as originating from the Z form present in the ground state in the BTN glass at 77 K due to either the temperature dependent L $\leftrightarrow$ Z equilibrium or, more likely, due to the Z form produced by the lactone ring opening as a result of interaction of the L molecule in the ground state with surfaces of solvent microcrystals or inhomogeneous sites existing at the glass cracks. A similar existence of the Z form in the ground state was reported for rigid solutions of the rhodamine 101 lactone in MTHF at 93 K, and this was associated with the optical condition of the glass, in particular the presence of cracks and traces of polycrystalline snow [21].

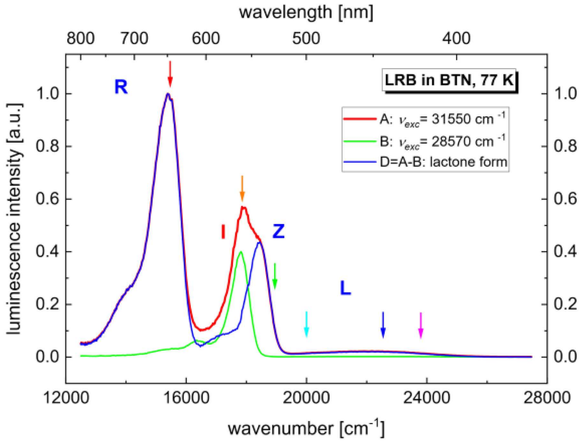

Fig. 3. Luminescence spectrum of a rigid solution of rhodamine B lactone in BTN at 77 K, recorded at $\tilde{\nu}_{exc} = 31550$ cm^{-1} (317 nm, red line) and corrected (blue line) by subtracting the fluorescence contribution from the directly excited coloured form recorded with an excitation energy beyond the lactone absorption spectrum at $\tilde{\nu}_{exc} = 28570$ cm^{-1} (350 nm, green line). The arrows indicate the wavenumbers for which the excitation spectra were recorded (see Fig. 4).

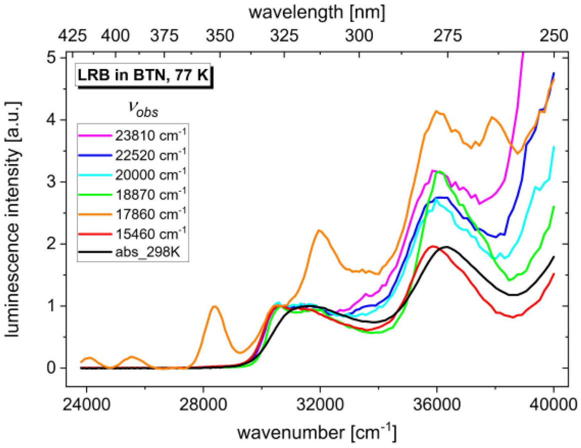

Fig. 4. Luminescence excitation spectra of 2.5×10^{-6} M LRB in BTN at 77 K, recorded across the luminescence spectrum at the wavenumbers as indicated by arrows in Fig. 3, and compared with the absorption spectrum at 298 K (black line).

The spectrum obtained after subtracting the 17850 cm^{-1} band (spectrum D = A − B, Fig. 3; the 18400 cm^{-1} band in the D spectrum is hereinafter referred to as the Z band) represents the luminescence generated upon photoexcitation of the L form in BTN. This origin is confirmed by the luminescence excitation spectra (shown in Fig. 4) recorded across the entire emission spectrum, at the wavenumbers indicated by arrows in Fig. 3, other than 17850 cm^{-1}.

Except for $\tilde{\nu}_{obs} = 17850$ cm^{-1}, all spectra match the band pattern and shape of the absorption spectrum recorded at 298 K (see Fig. 4), which proves that all three emission bands result from photoexcitation of the L form. The differences in the peak intensity ratios of the first (max. at 30600 cm^{-1}) and second (max. at 36000 cm^{-1}) bands in the excitation spectra reflect the excitation energy-dependent yields of the formation of the emitting states, which in turn must be related to the excitation-energy dependent rates of the processes leading to these states. It is to be noted that the luminescence excitation spectrum recorded for $\tilde{\nu}_{obs} = 17850$ cm^{-1} agrees well with the absorption spectrum of the colour form of RB in acetonitrile [9], which additionally confirms the assignment of the band peaking at 17850 cm^{-1} to the Z form.

3.3. Solvent effect at 77 K

Figure 5 (left) compares luminescence spectra of LRB in BTN, MTHF and MCH at 77 K. In all solvent glasses, three emission bands (i.e., L, Z, and R) from the photoexcited lactone molecule are observed. Unlike in BTN, no colour form is observed in MTHF at 77 K, which is likely due to the uncracked MTHF glass. In spite of similarly excellent glass quality, the luminescence spectra of rigid solutions of LRB in MCH at 77 K were found to depend significantly on the excitation energy, with the emission dominated by the I band peaking at 16750 cm^{-1} (597 nm). This band could also be excited by photon energies beyond the UV absorption spectrum of the L form and as such must come from a directly excited colour form of RB. This colour form may be produced due to a shift in the L ↔ Z equilibrium towards the Z form at 77 K, or due to trace protic impurities generating the C form. More likely, however, the colour form in MCH glass is produced by the opening of the lactone ring as a result of the ground-state interaction of the L molecule with the surface of the silica cell used for luminescence measurements [15]. For these reasons, we present only qualitative results for LRB in MCH at 77 K, mainly to indicate the presence of the Z and R bands also in this glass.

Table I presents the luminescence quantum yields in MTHF and BTN solutions at 298 K and glasses at 77 K (see also [35]). The quantum yield of total luminescence in MTHF glass, $\Phi_{\text{T-77K}}$, was determined using the procedure described earlier [28], with the assumption that the molar absorptivity of the L form at 77 K does not change, and that the only change in absorbance upon passing from solution at 298 K to solvent glass at 77 K is due to solvent contraction at 77 K. The change in the refractive index between 298 and 77 K was taken into account appropriately [28]. The partial quantum yields of L, Z, and R luminescence ($\Phi_{\text{L-77K}}$, $\Phi_{\text{Z-77K}}$, and $\Phi_{\text{R-77K}}$, respectively) were determined as the corresponding fractions of total luminescence intensity. Unlike as in MTHF, the quantum yield of the total luminescence in BTN at 77 K was determined by taking into account that in this glass, a significant fraction of the lactone molecules is converted into a colour form, which not only emits its own fluorescence in the band peaking at 17850 cm^{-1}, but also significantly depletes the population of the lactone molecules in the glass.

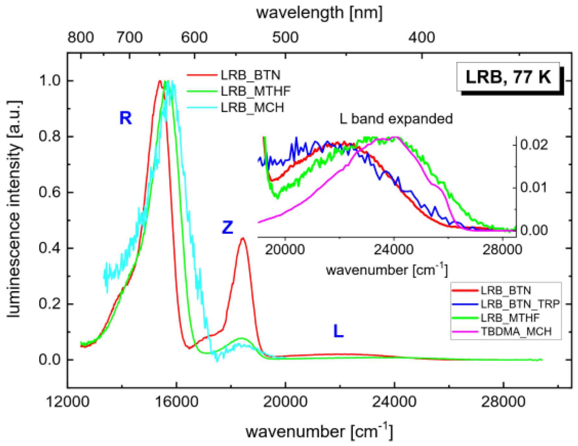

Fig. 5. Luminescence spectra of LRB in MCH, MTHF and BTN at 77 K and $\tilde{\nu}_{exc}$ = 32470 cm^{-1} (308 nm). Inset shows the expanded L band from the spectra in MTHF and BTN glasses compared to the gated phosphorescence spectrum (delay 0.5 ms, gate 10 ms) of LRB in BTN (blue) and to the gated (delay 0.1 ms, 50 ms gate) phosphorescence spectrum of TBDMA in MCH.

TABLE I

Quantum yields of total and band-related luminescences at 298 K and 77 K in MTHF and BTN.

Quantum yield	MTHF	BTN
$\Phi_{\text{L-298\,K}}{}^{a}$	0.07	0.01
$\Phi_{\text{Z-298\,K}}{}^{a}$	–	0.03
$\Phi_{\text{T-77\,K}}{}^{b}$	0.69	0.74
$\Phi_{\text{L-77\,K}}{}^{c}$	0.02	0.03
$\Phi_{\text{Z-77\,K}}{}^{d}$	0.05	0.18
$\Phi_{\text{R-77\,K}}{}^{e}$	0.62	0.53

[a] Fluorescence quantum yield at 298 K;
[b] Quantum yield of total luminescence at 77 K;
[c] Quantum yield of luminescence at 77 K in the L band;
[d] Quantum yield of luminescence at 77 K in the Z band;
[e] Quantum yield of luminescence at 77 K in the R band.

Decreasing the temperature from 298 to 77 K and passing to a solid glass environment result in dramatic changes in the quantum yield and decay times of the total luminescence of LRB. A significant effect of the type of solvent glass is also observed. In both examined glasses, the quantum yield of total emission is very high (0.74 and 0.69 in BTN and MTHF, respectively, Table I) and indicates that all products of excited-state processes in LRB are visualized by their luminescence. The emissions displayed in individual bands differ significantly in their components, intensities, quantum yields and decay times. Unlike at 298 K, where the L band comprises only fluorescence from the highly polar ^{1}L$_{\text{CT}}$ state, in BTN at 77 K the L band includes a short-lived ns fluorescence and, in addition, a long-lived emission that decays on the microsecond time scale (Table II). This long-lived component is interpreted as phosphorescence originating from the charge transfer triplet state of the L form, ^{3}L$_{\text{CT}}$. This assignment is supported by comparison of the steady-state L band with time-resolved phosphorescence spectra of LRB in BTN at 77 K, one of which, recorded with a 0.5 ms delay and a 10 ms gating, is shown in Fig. 5. In view of a very low energy gap between the ^{1}L$_{\text{CT}}$ and ^{3}L$_{\text{CT}}$ states, the emission

TABLE II

Decay parameters of LRB luminescence in MTHF and BTN at 298 K and 77 K.

Decay parameters	MTHF	BTN
298 K, Fl	21280 cm^{-1f}	20840 cm^{-1}
$\tau_{\text{L-298K}}{}^{a}$ [ns]	17.8	6.6
298 K, Fl		17860 cm^{-1}
$\tau_{\text{Z-298K}}{}^{b}$ [ns]	–	0.8
77 K, L band, Fl	22220 cm^{-1}	21280 cm^{-1}
$\tau_{\text{L-Fl-1}}{}^{c}$ [ns]	2.3	2.9
$Q_{\text{L-Fl-1}}{}^{d}$ [%]	58	21
$\tau_{\text{L-Fl-2}}{}^{c}$ [ns]	10.2	16.7
$Q_{\text{L-Fl-2}}{}^{d}$ [%]	42	79
$\tau^{av}_{\text{L-Fl-77K}}{}^{e}$ [ns]	3.4	8.2
77 K, Z band, Fl	18520 cm^{-1}	18870 cm^{-1}
$\tau_{\text{Z-Fl-77K}}{}^{c}$ [ns]	2.1	2.8
77 K, L band, Ph		21740 cm^{-1}
$\tau_{\text{L-Ph-1}}{}^{c}$ [μs]		5.0 ^{g}
$\tau_{\text{L-Ph-2}}{}^{c}$ [μs]		18.7 ^{g}
77 K, R band, Ph	15630 cm^{-1}	15380 cm^{-1}
$\tau_{\text{R-Ph-1}}{}^{c}$ [s]	0.09	0.28
$Q_{\text{R-Ph-1}}{}^{d}$ [%]	50	42
$\tau_{\text{R-Ph-2}}{}^{c}$ [s]	0.22	0.65
$Q_{\text{R-Ph-2}}{}^{d}$ [%]	50	58
$\tau^{av}_{\text{R-Ph-77 K}}{}^{e}$ [s]	0.13	0.42

[a] Fluorescence decay time in L band at 298 K;
[b] Fluorescence decay time in Z band at 298 K, after separation of the overlap with the L band;
[c] Fluorescence (Fl) or phosphorescence (Ph) decay times from 2-exponential fit of the decay in the L or Z band and a band at 77 K;
[d] Component contribution (relative amplitude [in %]) to the decay $Q_i = a_i\tau_i / \sum_i a_i\tau_i$ in multiexponential fit;
[e] Amplitude average fluorescence decay time $\tau_F^{av} = \sum_i a_i\tau_i / \sum_i a_i$ [35];
[f] Wavenumber at which the luminescence decay was recorded;
[g] Two of three components in 3-exponential decay.

spectra from these states are expected to be very similar, which explains the near-identity of the gated phosphorescence and steady-state spectra. A similar coexistence of CT fluorescence and CT phosphorescence was reported for the structurally related malachite green lactone [6] At present, we are not able to quantitatively estimate the contributions of each of these two emissions to the L band of LRB.

Similarly, the L band in MTHF at 77 K comprises a long-lived component, and its similarity with TBDMA phosphorescence (Fig. 5, inset) might suggest that both the emitting triplet and its population mechanism are different than in BTN. However, further properties of the long-lived states emitting in the L band require more detailed examination, and research towards a better understanding of the intersystem crossing mechanism generating the $^3\text{L}_{\text{CT}}$ state is currently underway.

Based on the luminescence decays (see Sect. 3.4 below) and the data reported earlier for LR101 [21], the short-lived Z and the long-lived R bands in LRB spectra recorded at 77 K are interpreted as fluorescence and phosphorescence, respectively. The higher quantum yields determined for these bands indicate that processes related to generation of the excited ring-open forms are much more efficient than ISC, which results in the population of the $^3\text{L}_{\text{CT}}$ state and account for more than 2/3 of the entire deactivation in both solvent glasses (see Table I). The large difference in $\Phi_{\text{Z-77 K}}$ (0.05 in MTHF vs 0.18 in BTN) and in $\Phi_{\text{R-77K}}$ (0.62 in MTHF vs 0.53 in BTN) reveals a significant effect of the type of glass on the excited state branching, and in fact on the intramolecular charge separation and recombination. A similar effect on the solvent glass was observed for the malachite green lactone analogue [28].

3.4. Luminescence decays at 77 K

The luminescence decay curves recorded for LRB in BTN at 77 K in the L, I and R bands extend over multiple time scales from nanoseconds to seconds due to the overlap of short-lived (~ ns) fluorescence components and long-lived (μs to s) phosphorescence components. The fluorescence decays recorded in the L and I bands are presented in Fig. 6, while the phosphorescence decays recorded in the R band are shown in Fig. 7. The decay times obtained from multiexponential fitting of the luminescence decay curves collected in these bands are presented in Table II. No short-lived component is observed in the R band, and only a constant background has been recorded on the ns time scale. A long-lived constant background resulting from the overlap with the long-lived phosphorescence occurs also in the fluorescence decays recorded in the L bands, and, though to a much lesser extent, in the I and Z bands, and must have been subtracted in order to extract the short-lived decays on the ns time scale.

The fluorescence decays recorded in the I band for the Z form excited directly from the ground state (emission at 17850 cm^{-1}) and that populated upon excitation of the L form (emission at 18400 cm^{-1}) show no rise time and could be fitted with a monoexponential decay function. Interestingly, the decay time of the fluorescence from the directly excited Z form is longer (3.3 ns) than that of the Z form generated in the excited state (2.8 ns). Nevertheless, the values of 2.8 or 3.3 ns are substantially lower than

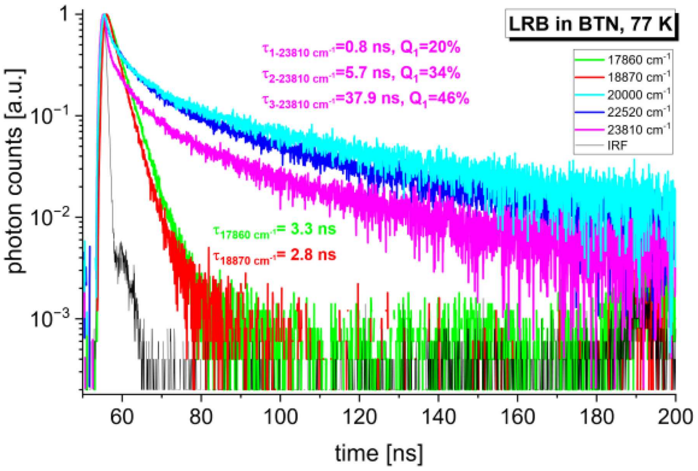

Fig. 6. Fluorescence decays of LRB in BTN at 77 K recorded in the L and I bands, at $\tilde{\nu}_{exc} = 33000$ cm^{-1} (303 nm), together with the decay times (τ) and the component contributions (Q_i) in the multiexponential fitting.

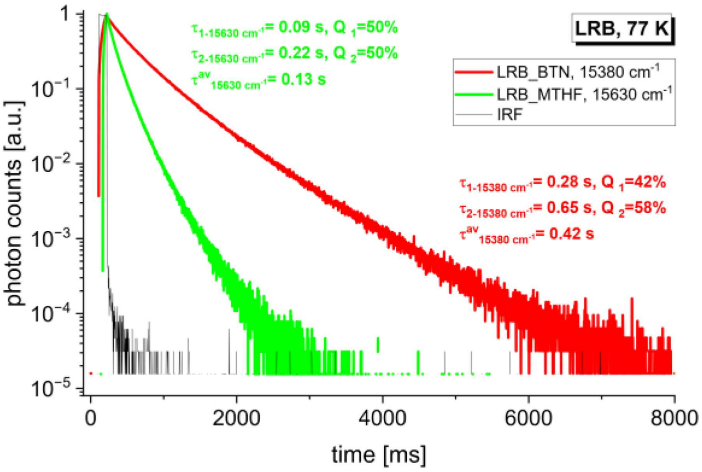

Fig. 7. Phosphorescence decays of LRB in MTHF and BTN at 77 K recorded in the R band, at $\tilde{\nu}_{exc} =$ 32680 cm^{-1} (306 nm), together with the decay times (τ), the component contributions (Q_i), and the average decay time (τ^{av}) obtained in the multiexponential fitting.

the fluorescence decay time of 5.3 ns reported for RB in ethanol–glycerol at 77 K [36], thus indicating an enhanced nonradiative deactivation process both in the Z form present in the ground state and that photogenerated in LRB at 77 K.

On the other hand, the decay curves of both L fluorescence and phosphorescence are highly non-exponential and depend on the energy of emission transition (Fig. 6). The higher energy fluorescence emitted in the blue part of the L band decays faster than the fluorescence monitored on the red side. We have verified that the glassy solvent matrix does not contribute to the fluorescence decays. Though a coarse biexponential fitting (Table II) may suggest a biphasic deactivation process, we hypothesise that the non-exponentiality of the fluorescence and phosphorescence decays in the L band is in fact more complicated (see the decay times for $\tilde{\nu}_{em} = 23810$ cm^{-1} recovered from the 3-exponential fit given in Fig. 6) and reflects, e.g. a non-uniform distribution of molecular geometries of LRB or of solvent sites around the LRB molecule.

The phosphorescence decays recorded in the R band are non-exponential and extend on the s time scale (Fig. 7). As in the case of L fluorescence, the observed non-exponential character likely reflects the heterogenicity of molecular geometry distributions of LRB. Most probably, the effect of the environment is smaller, because the shape and position of the R band only slightly depend on the type of glass. The effect of the molecular geometry of the emitting triplet state finds support in the large difference in the radiative decay of the R band between MTHF and BTN, which in the case of in the former solvent is more than 3 times faster, with $\Phi_{\text{R-77K}}$ in MTHF distinctly greater than that in BTN.

4. Discussion

In low-temperature absolute ethanol glass, the Z form of RB displays fluorescence with a quantum yield of nearly 1.0 [37]. This means that under conditions when the carboxylphenyl group of RB is effectively hydrogen-bonded to the solvent molecule(s), the xanthene chromophore of RB is stabilized and does not deactivate by nonradiative processes. The intersystem crossing is inactive and the triplet state is not populated. At higher temperatures, when the hydrogen bonding is less stable [38] or in the absence of hydrogen bonding, for instance when adsorbed on the surfaces of the organic crystals, the xanthene chromophore of RB shows both a reduced fluorescence quantum yield and lifetime [39]. Enhanced nonradiative deactivation of rhodamines has been related by Kemnitz et al. [40] with significant geometry changes within the xanthene moiety, consisting in a butterfly-like motion of the two halves of the molecule along the short axis. Based on a theoretical modelling, Obukhova et al. [31] reached similar conclusion in relation to LRB, proposing that the large Stokes shift of LRB in nonpolar solvents results from the excited-state structural relaxation process consisting in out-of-plane deformation of the initially planar xanthene moiety.

In rhodamines, the triplet state has been quite rarely included in the description of the radiationless process [41]. Other studies seem to contradict this, pointing to very low triplet yields [42, 43] (e.g. for RB ranging from 0.003 to 0.006 in protic solvents) and indicating that intersystem crossing seems to play a minor role in the degradation of excitation energy in rhodamines. There are only very few reports investigating phosphorescence of rhodamines [44, 45]. On the other hand, our study reporting the phosphorescence of LR101 [21] showed that triplet states play a significant role in the deactivation of rhodamine lactones. A large presence of long-lived triplet states in LRB was also preliminarily reported based on transient absorption measurements of LRB [46, 47]. We originally proposed that the highly efficient emitting triplet state is the triplet state of the Z form [21]. Based on our findings from this study, we tend to revise this assignment and relate the phosphorescence observed for LR101 and reported for LRB in this study to the triplet state of a triarylmethane-like quinoid form, (^{3}Z$_1$), generated on the relaxation pathway of the vibrationally excited open-ring anion.

The complex photophysical processes in LRB (Fig. 8) can be rationalized by taking into account that the driving force for the ultrafast charge separation (CS) from the photoexcited Franck–Conden state, ^{1}L$_{\mathrm{FC}}$, to the non-relaxed charge transfer state, [^{1}L$_{\mathrm{CT}}$]*, in rigid medium may be provided by the high dipole moment of the PD moiety (4.9 D) [48]. This moiety acts as a chemical dipole trap [49], capturing an electron from the xanthene part. Phthalide is known to capture low-energy electrons in the gas phase via a shape-resonance state, which rapidly relaxes to the vibrationally excited closed-ring and open-ring molecular anions. Both deactivation channels to relaxed bicyclic and open-ring structures start from a vibrationally excited state of the anion and compete with each other. The phthalide anion can exist in two stable structures, namely one short-lived and close to the bicyclic geometry of the neutral molecule, and the other long-lived with a five-membered lactone ring open by cleavage of the C–O bond [50].

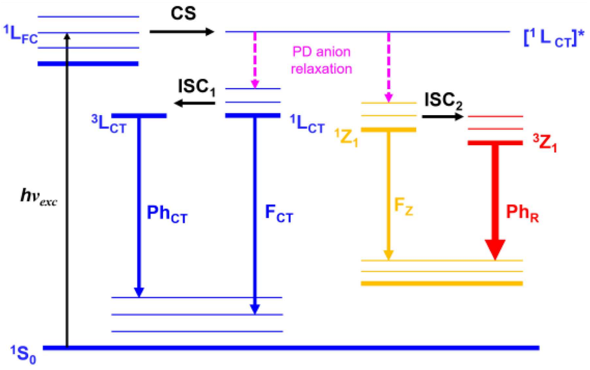

Fig. 8. Energy diagram for LRB.

Ultrafast photoinduced ET in LRB in a rigid solvent glass can be envisaged as electron capture from the DEA Rydberg orbital by phthalide acting as a dipole trap, and the successive photophysics is controlled by the interplay of intramolecular anion relaxation with local electric fields in the solvent glass. The rigid environment does not only distort the field created by the dipole, thereby affecting the ET process, but further must affect the excited state, branching into pathways leading to the emitting products. Subsequently, the further fate of the system would depend on the capability of the glass to screen or shield the electric interactions between electron-donating and electron-accepting moieties in the LRB molecule.

5. Conclusions

Ultrafast photoinduced intramolecular electron transfer in spirocyclic rhodamine lactones is driven by local electric fields with strong contribution of the electron-accepting phthalide moiety, which plays the role of a dipole trap capturing electron via a shape resonance state involving selective vibrational excitation of the C–O bond in phthalide. This resonance state relaxes rapidly to two structurally different, stable phthalide molecular anions with a closed and an open lactone ring. In this study, we explored the subsequent relaxation of excited lactone molecules with these different acceptor anions in an organic solvent glasses at 77 K and observed dual fluorescence and dual phosphorescence. The two fluorescence bands are assigned to the ^{1}CT state of the closed ring form and the S_1 state of the zwitterion form, respectively. The short-wave phosphorescence band in butyronitrile is assigned to triplet charge transfer, while the other intense long-wave red band is tentatively assigned to the triplet state of the triarylmethane-like quinoid form. The CT triplet emitting phosphorescence in the L band is produced in a $^1L_{CT} \rightarrow {}^3L_{CT}$ intersystem crossing mechanism. The red emitting triplet is produced independently from the open-ring anion, and the exploration of its formation mechanism is currently underway. The organic solvent glasses play important role in the intramolecular electron transfer processes in rhodamine lactones by providing the solute environment with local electric fields that actively influence the electric interaction between the electron-donating and electron-accepting moieties of the LRB molecule.

Acknowledgments

This work has been supported by the statutory funds of the Institute of Physics, Polish Academy of Sciences.

References

[1] H.J. Feng, M.-J. Zhang, L.-H. Jiang, L. Huang, D-W. Pang, *Acc. Chem. Res.* **58**, 3543 (2025).

[2] J.W. Verhoeven, *J. Photochem. Photobiol. C* **7**, 40 (2006).

[3] Y. Liu, G. Zhan, Z.-W. Liu, Z.-Q. Bian, C.-H. Huang, *Chin. Chem. Lett.* **27**, 1231 (2016).

[4] A. Rao, P.C.Y. Chow, S. Gélinas, C.W. Schlenker, C.-Z. Li, H.L. Yip, A.K.-Y. Jen, D.S. Jen, R.H. Friend, *Nature* **500**, 435 (2013).

[5] D.J. Gibbons, A. Farawar, P. Mazzella, S. Leroy-Lhez, R.M. Williams, *Photochem. Photobiol. Sci.* **19**, 136 (2020).

[6] J. Karpiuk, *Phys. Chem. Chem. Phys.* **5**, 1078 (2003).

[7] T. Bizjak, J. Karpiuk, S. Lochbrunner, E. Riedle, *J. Phys. Chem. A* **108**, 10763 (2004).

[8] E. Noelting, K. Dziewoński, *Ber. Dtsch. Chem. Ges.* **38**, 3516 (1905).

[9] D.A. Hinckley, P.G. Seybold, D. Borris, *Spectrochim. Acta* **42A**, 747 (1986).

[10] M. Beija, C.A.M. Afonso, J.M.G. Martinho, *Chem. Soc. Rev.* **38**, 2410 (2009).

[11] K.H. Drexhage, in: *Dye Lasers*, Ed. Fritz Peter Schäfer, Springer, Berlin, Heidelberg 2005, p. 155.

[12] X. Chen, T. Pradhan, F. Wang, J.S. Kim, J. Yoon, *Chem. Rev.* **112**, 1910 (2012).

[13] S. Zeng, X. Liu, Y.S. Kafuti, H. Kim, J. Wang, X. Peng, H. Li, J. Yoon, *Chem. Soc. Rev.* **52**, 5607 (2023).

[14] K. Kolmakov, V.N. Belov, J. Bierwagen, C. Ringemann, V. Müller, C. Eggeling, S.W. Hell, *Chem. Eur. J.* **16**, 158 (2010).

[15] M.J. Snare, F.E. Treloar, K.P. Ghiggino, P.J. Thistlethwaite, *J. Photochem.* **18**, 335 (1982).

[16] F. López Arbeloa, T. López Arbeloa, M.J. Tapia Estévez, *J. Phys. Chem.* **95**, 2203 (1991).

[17] V.E. Korobov, V.V. Shubin, A.K. Chibisov, *Chem. Phys. Lett.* **45**, 498 (1977).

[18] A. Dunne, M.F. Quinn, *J. Chem. Soc. Faraday Trans. 1* **73**, 1104 (1977).

[19] P.C. Beaumont, D.G. Johnson, B.J. Parsons, *J. Photochem. Photobiol. A* **107**, 175 (1997).

[20] U.K.A. Klein, F.W. Hafner, *Chem. Phys. Lett.* **43**, 141 (1976).

[21] J. Karpiuk, Z.R. Grabowski, F.C. De Schryver, *J. Phys. Chem.* **98**, 3247 (1994).

[22] T.M. Grigoryeva, V.L. Ivanov, N. Nizamov, M.G. Kuzmin, *Dokl. Akad. Nauk SSSR* **232**, 1108 (1977).

[23] J. Karpiuk, Z.R. Grabowski, F.C. De Schryver, *Proc. Indian Acad. Sci. Chem. Sci.* **104**, 133 (1992).

[24] J. Karpiuk, *J. Luminesc.* **60–61**, 474 (1994).

[25] K. Veys, D. Escudero, *Acc. Chem. Res.* **55**, 2698 (2022).

[26] J. Karpiuk, *Phys. Chem. Chem. Phys.* **5**, 1078 (2003).

[27] J. Karpiuk, E. Karolak, J. Nowacki, *Pol. J. Chem.* **82**, 865, (2008).

[28] J. Karpiuk, A. Majka, E. Karolak, J. Nowacki, *J. Phys. Chem. Lett.* **8**, 4659 (2017).

[29] A.A. El-Rayyes, A.A. Al-Arfaj, U.K.A. Klein, S.A.I. Barri, *Catal. Lett.* **97**, 83 (2004).

[30] A.N. Sinel'nikov, V.Ya. Artyukhov, *Russ. J. Phys. Chem. A* **87**, 1409 (2013).

[31] O.M. Obukhova, N.O. Mchedlov-Petrossyan, N.A. Vodolazkaya, L.D. Patsenker, A.O. Doroshenko, *Colorants* **1**, 58 (2022).

[32] X. Wang, M. Song, Y. Long, *J. Solid State Chem.* **156**, 325 (2001).

[33] J. Karpiuk, P. Gawryś, E. Karpiuk, K. Suwińska, *Chem. Commun.* **55**, 8414 (2019).

[34] J. Karpiuk, *J. Phys. Chem. A* **108**, 11183 (2004).

[35] A. Stillen, Y. Engelborghs, *Photochem. Photobiol.* **67**, 475 (1998).

[36] R.W. Chambers, T. Kajiwara, D.R. Kearns, *J. Phys. Chem.* **78**, 380 (1974).

[37] T. Karsten, K. Kobs, *J. Phys. Chem.* **84**, 1871 (1980).

[38] R.F. Kubin, A.N. Fletcher, *J. Luminesc.* **27**, 455 (1982).

[39] I. López-Arbeloa, K.K. Rohatgi-Mukherjee, *Chem. Phys. Lett.* **129**, 607 (1986).

[40] K. Kemnitz, N. Tamai, I. Yamazaki, N. Nakashima, K. Yoshihara, *J. Phys. Chem.* **91**, 1423 (1987).

[41] H. Alobaldi, F. Alberkdar, Z. Hafidh, S. Alalkway, in: *Laser-Induced Processes in Molecules* Eds. K.L. Kompa, S.D. Smith, Springer, Berlin 1979, p. 108.

[42] V.E. Korobov, U.V. Shubin, A.K. Chibisov, *Chem. Phys. Lett.* **45**, 498 (1977).

[43] A.K. Chibisov, H.A. Kezle, L.V. Levshin, T.D. Slavnova, *J. Chem. Soc. Chem. Commun.*, 1292 (1973).

[44] R.W. Chambers, D.R. Kearns, *J. Phys. Chem.* **72**, 4718 (1968).

[45] R.N. Nurmukhametov, N.I. Kunavin, G.T. Khachaturova, *Izvest. Akad. Nauk SSSR Ser. Fiz.* **42**, 517 (1978).

[46] J. Jasny, J. Sepioł, J. Karpiuk, J. Gilewski, *Rev. Sci. Instrum.* **65**, 3646 (1994).

[47] J. Karpiuk, Z.R. Grabowski, *AIP Conf. Proc.* **364**, 91 (1996).

[48] I. Wallmark, M.H. Krackov, S.-H. Chu, H.G. Mautner, *J. Am. Chem. Soc.* **92**, 4447 (1970).

[49] N.M. Shishlov, S.L. Khursan, *Russ. Chem. Bull. Int. Ed.* **64**, 766 (2015).

[50] N.L. Asfandiarov, S.A. Pshenichnyuk, A.S. Vorob'ev, E.P. Nafikova, A.N. Lachinov, V.A. Kraikin, A. Modelli, *J. Chem. Phys.* **142**, 174308 (2015).